



Non-invasive three-dimensional bone–vessel image fusion using black bone MRI based on FIESTA-C



T. Hayashi^a, N. Fujima^{b,*}, A. Hamaguchi^a, T. Masuzuka^a, K. Hida^a, S. Kodera^b

^a Department of Radiology, Sapporo Azabu Neurosurgical Hospital, Sapporo, Japan

^b Department of Diagnostic and Interventional Radiology, Hokkaido University Hospital, Sapporo, Japan

ARTICLE INFORMATION

Article history:

Received 14 February 2018

Accepted 24 December 2018

AIM: To evaluate the image quality of bone–vessel fused volume-rendering (VR) images reconstructed by three-dimensional “black bone” magnetic resonance imaging (MRI) based on the fast imaging employing steady-state acquisition cycled phases (FIESTA-C) sequence and time-of-flight magnetic resonance angiography (TOF-MRA).

MATERIALS AND METHODS: Seventeen patients were analysed in this retrospective study. All patients underwent both MRI techniques including FIESTA-C and TOF-MRA and computed tomography angiography (CTA). MRI- and CT-based bone–vessel VR images were reconstructed. Visual depictions of frontal and parietal branches from the superficial temporal artery (STA) were independently scored by three experienced radiological technologists using a four-grade system.

RESULTS: In the visual evaluation, the scores of the both right and left frontal branches in MRI-based VR image were significantly larger those at CT ($p < 0.01$, respectively). The scores of both the right and left parietal branches tended to be larger in MRI-based than that in CT-based VR imaging, but were not significantly so ($p = 0.06$, 0.13 respectively). In the interobserver agreement analysis, κ values were all good (range: $0.6–0.76$) for STA branch evaluation in MRI-based VR images.

CONCLUSION: MRI bone–vessel fused VR imaging can non-invasively depict STA frontal branches with better visibility compared to the CT-based VR imaging. This technique may be useful for the preoperative evaluation of donor branches for STA–middle cerebral artery bypass surgery.

© 2019 The Royal College of Radiologists. Published by Elsevier Ltd. All rights reserved.

Introduction

External carotid artery–internal carotid artery (ECA-ICA) bypass is an important treatment method in cases of intracranial vascular occlusion or stenosis such as Moyamoya disease.^{1–3} In particular, superficial temporal artery (STA)–middle cerebral artery (MCA) bypass surgery is

* Guarantor and correspondent: N. Fujima, Department of Diagnostic and Interventional Radiology, Hokkaido University Hospital, N15, W7, Kita-Ku, Sapporo 060-8638, Japan. Tel.: +81 11 706 5977; fax: +81 11 706 7876.

E-mail address: Noriyuki.Fujima@mb9.seikyone.jp (N. Fujima).

frequently performed. Three-dimensional (3D) computed tomography (CT) angiography (CTA) is usually used to evaluate potential donor branches of the ECA for ECA-ICA bypass using reconstruction of the volume-rendering (VR) image of arteries running along the surface of the skull; however, poor depiction of the ECA branches in CTA is sometimes experienced, probably because of the mismatch between image acquisitions and transit delay in the contrast agent and the beam-hardening effect due to the high attenuation values of the skull. ECA branches are particularly sensitive to these effects because these arteries are usually running along the surface of the skull, resulting in their poor depiction on imaging. Furthermore, there are several risks related to the invasiveness of CTA: allergies to iodine contrast agent, extravascular leak due to too-rapid injection, and radiation exposure.⁴

In contrast, time-of-flight (TOF) magnetic resonance angiography (MRA) can be used to visualise intra- and extracranial arteries non-invasively. In recent decades, the image quality and arterial depiction of TOF-MRA has been developing,⁵ with the broad spread of 3 T magnetic resonance imaging (MRI) units worldwide. Using arteries that are well depicted by TOF-MRA, the preoperative evaluation of ICA and ECA for ECA-ICA bypass surgery can be performed non-invasively; however, there remains one problem: the reconstruction of VR images with both vessel and bone depiction is difficult using MRI only, because MRI is not suitable for composing 3D skull images. To solve this problem, previous studies have performed 3D image reconstruction of the skull utilising the low signal intensity of the bone acquired by gradient echo sequences, also known as the “black bone” MRI.^{6–11} The aim of the present study was to evaluate the clinical utility of bone–vessel VR images reconstructed using MRI 3D skull imaging and TOF-MRA.

Materials and methods

Patients

The protocol of this retrospective study was approved by the institutional review board, and written informed consent was waived. Seventeen patients who were surgically treated with ECA-ICA bypass at Sapporo Azabu Neurosurgical Hospital from November 2015 to May 2016 were evaluated. Patient characteristics were as follows: seven men and 10 women, average age 51.14 (range, 25–67) years. In the preoperative evaluation, all patients underwent magnetic resonance imaging (MRI) including 3D fast imaging employing steady-state acquisition cycled phases (FIESTA-C) and TOF-MRA. All patients also received CTA before the preoperative MRI evaluation mentioned above.

Imaging protocol

MRI was performed using a 3 T magnet (Discovery MRI 750, GE Healthcare, Milwaukee, MI, USA) with a 12-inch head neck and spine coil. Post-processing of VR reconstruction was performed by ZIO Workstation (ZIOSOFT, Tokyo, Japan). In previous reports, so-called “black-bone”

MRI was developed using the 3D volume of proton-weighted image contrast for good depiction of bone tissue with low signal intensity.^{6–9} In the present study, the FIESTA-C sequence was used in the acquisition of black-bone MRI raw images for both the short scanning time and a high signal-to-noise ratio (SNR). In the image acquisition, because the black-bone MRI utilised the black signal intensity from cortical bone to depict the bone surface structure, the partial volume effect of yellow bone marrow high signal intensity sometimes obstructs this black-bone signal. Sites where cortical bone is very thin (such as temporal bone) may be largely influenced by this partial volume effect of high signal intensity in yellow bone marrow. This will result in poor depiction of black-bone MRI after VR processing. It was thus necessary to suppress the high signal of marrow fat as much as possible. It was also necessary to prevent the banding artefacts, which are specific to the balanced steady-state free precession (b-SSFP) sequence.^{12,13} In light of these findings, the following parameter settings have been used as the basic acquisition scheme for black-bone MRI at Sapporo Azabu Neurosurgical Hospital¹: the imaging parameters of shortest repetition time (TR) and echo time (TE) were used for fast acquisition,² an intermediate-value flip angle (FA) of 17° was used to obtain images with an only-intermediate marrow fat signal and to reduce the degree of the banding artefacts.^{12,13} Details of the imaging parameters of black-bone MRI used in the current study are summarised in Table 1. TOF-MRA was also obtained with the following parameters: TR=23 ms, TE=3.4 ms, flip angle=18°, field of view=20 cm, matrix=448 × 224, section thickness=1 mm, number of sections=168. In addition, CTA was performed in all patients using a 64-slice multidetector-row CT system (Light Speed VCT Vision, GE Healthcare, Milwaukee, WI, USA). The settings used for CT were as follows: 120 kVp, 800 mA, 0.4 s/rot, and helical pitch = 0.53. Before the scanning, 350 mg iodine contrast agent (iopamidol, 370 mg iodine/ml, Bayer, Osaka, Japan) was intravenously injected by power injector with the flow rate of 29.2 mg iodine/kg/s (12-second injection). Arterial arrival of the contrast agent for the determination of acquisition timing was adjusted for the depiction of intracranial arteries using a bolus-tracking technique with the target point being the distal ICA. All imaging was performed to include the whole brain in its scan range.

Table 1

Parameters for the acquisition of three-dimensional fast imaging employing steady-state acquisition cycled phases (FIESTA-C).

Matrix	384×320
Field of view (cm)	22
Section thickness (mm)	1.4
TR (ms)	4.6–4.8
TE (ms)	1.7–1.8
Bandwidth (kHz)	90.91
Number of sections	200
Zip	2
ARC factor	1.75×1.75
Scan time	3 min 3 s

ZIP, zero fill interpolation; ARC, autocalibrating reconstruction for Cartesian imaging (phase×slice).

Post-processing

Post-processing was performed to create 3D bone–vessel fusion images from TOF-MRA and black-bone images obtained by 3D FIESTA-C sequences in all patients using the VR technique. First, 3D image reconstruction was performed by the VR technique from raw image data of 3D FIESTA-C. In this process, window level and width were adjusted visually and manually so that the surface shape of soft tissue along the overall head and face could be recognised. Next, the whole volume of the VR image was inverted from black to white. By doing this, the signal intensity in the cortical bone was converted from black bone to high-signal-intensity bright bone. Similarly, the signal intensity of the air spaces was also converted to a high-signal-intensity area. As a result, both air and cortical bone were inverted to strong bright-white intensity, whereas the soft tissue along the face and head became a black signal. Next, by cutting out the bright signal intensity area of air (the outermost layer in 3D volume) in a manual fashion, a 3D bone image could be successfully obtained. In this process, the manual procedure was easily performed in all cases because the three layers—air (the outermost layer), facial soft tissue (the gap area between air and cortical bone), and bone surface—were clearly divided by their different signal intensities. This whole bone reconstruction process is summarised in Fig 1. An example 3D-bone image is presented in Fig 2. A 3D Advantage Workstation VolumeShare 5 (GE Healthcare) was used for the image fusion of the acquired black-bone MRI from FIESTA-C and the arterial vessel image from TOF-MRA. An autofusion algorithm was used with automatic adjustment of the field of

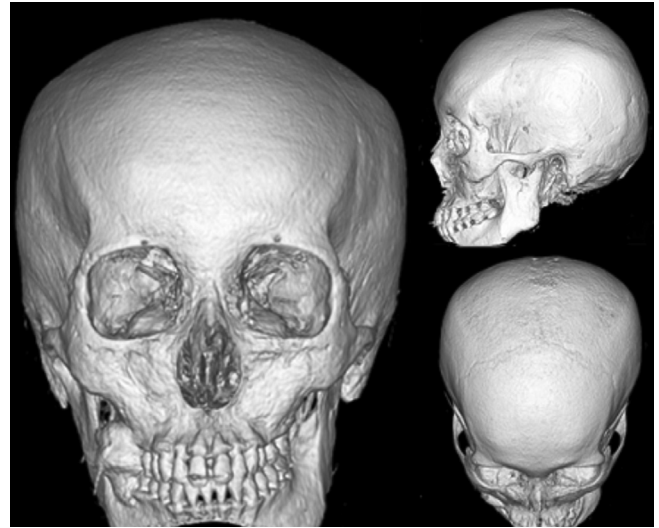


Figure 2 MRI-reconstructed 3D-volume rendering skull image. Example of a 3D VR bone–vessel fused image obtained from the FIESTA-C sequence. Clear depictions of the bone structure were observed from all three directions.

view and position information to overlay the TOF-MRA image onto the FIESTA-C based black-bone image. If necessary, a manual procedure was used for the adjustment of the overlay image location by moving and rotating the images. In addition, 3D VR imaging with both vessel and bone depiction from the 3D-CTA dataset was also created using the traditional VR technique with the threshold processing method.¹⁴ All 3D reconstruction procedures in both CT and MRI were

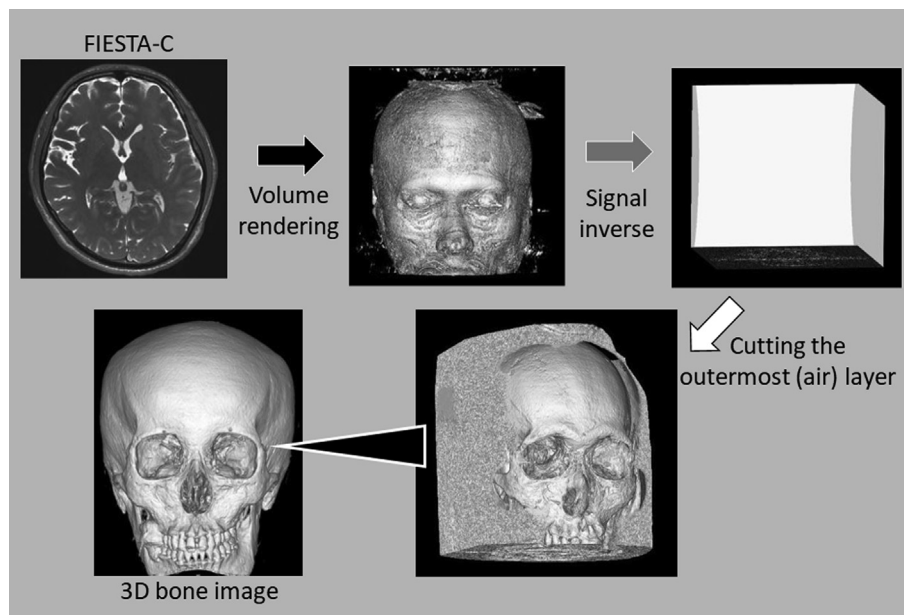


Figure 1 3D-reconstruction process of the black bone MRI. First, 3D image was reconstructed with the VR process from raw image data of 3D FIESTA-C (black arrow). Next, the whole volume of the VR image was inverted from black to white (grey arrow). After this process, both air and cortical bone were inverted to strong bright-white intensity, whereas the soft tissue along the face and head became a black signal. The bright signal intensity area of air (the outermost layer in 3D volume) was carefully cut with manual fashion (white arrow), a 3D bone image could be obtained (arrowhead).

performed to visualise vessel and bone structure as clearly as possible, in the typical clinical manner.

Visual evaluation

After randomising all MRI and CT based bone–vessel VR images, the degree of visualisation of the STA branches on each VR image was evaluated independently by three radiological technologists with 14, 20, and 25 years of experience, respectively. The depiction of STA was determined based on a four-grade system. Each grade was explained as follows: 0, almost no depiction; 1, only the proximal portion was depicted; 2, all portions were depicted, but the depiction of the distal portion was observed to be weak; 3, all parts were well depicted. Representative cases are presented in Fig 3 and were given to the scorers as references. Evaluated vessels were the four major STA branches: the right frontal, left frontal, right parietal, and left parietal. In each branch, the mean score of the three evaluators for each technique was calculated. To avoid any bias in the scoring of different images, those who had no experience of MRI-based vessel bone fusion images were chosen as raters. Additionally, they were blind to all information, including study purpose, and were simply asked to score the depiction of arteries without any other information.

Statistical analysis

Visual scores of each STA branch (right frontal, left frontal, right parietal, and left parietal branch) by the bone–vessel VR images obtained by MRI and CT techniques were compared using the Wilcoxon signed-rank test. In addition, interobserver agreement in all pairs among the three radiological technologists was analysed using kappa (κ) statistics, with the following criteria: 0–0.2, poor agreement; 0.21–0.4, fair agreement; 0.41–0.6, moderate agreement; 0.61–0.8, good agreement; 0.81–1.0, excellent agreement. The level of statistical significance was set at $p < 0.05$.

Results

All VR processing using 3D FIESTA-C and TOF-MRA was performed, resulting in coherent 3D bone–vessel VR images for all patients. In the visual score comparison of MRI- and CT-based bone–vessel VR images of STA branches, the score of right frontal branch MRI-based VR image (2.2 ± 0.9) was significantly larger than that for the respective CT image (1.8 ± 0.7 ; $p < 0.01$). The score of the left frontal branch VR image was also larger for MRI than CT (1.9 ± 0.7 versus 1.3 ± 0.8 ; $p < 0.01$). The score of both right and left parietal branches tended to be larger for MRI-based than CT-based VR images, but not significantly so ($p = 0.06, 0.13$, respectively). A summary of the comparison of visual scores is presented in Table 2. As a detail of the data, all scores in three raters for all the patients were presented in Electronic Supplementary Material, Tables S1–S4. Representative images highlighting marked differences in STA branch depiction between VR images based on MRI and CT are presented in Fig 4. In addition, the other nine cases with various degrees of difference in STA branch depiction are presented in Fig 5.

In the interobserver agreement analysis, κ values for STA branch evaluation in MRI-based VR images were all good. In CT-based VR images, the κ value for the evaluation of three branches (right frontal, right and left parietal branch) was good (0.60–0.76), but only a moderate κ value (0.5) was observed in the evaluation of the left frontal branch. All κ values are summarised in Table 3.

Table 2

Scores in the visual evaluation of superficial temporal artery branches.

Name of branch	CT	MRI
Right frontal branch	1.8 ± 0.7	2.2 ± 0.9^a
Left parietal branch	1.8 ± 1.0	2.1 ± 0.8
Right frontal branch	1.3 ± 0.8	1.9 ± 0.7^a
Left parietal branch	2.5 ± 0.6	2.6 ± 0.7

^a $p < 0.05$.

CT, computed tomography; MRI, magnetic resonance imaging.

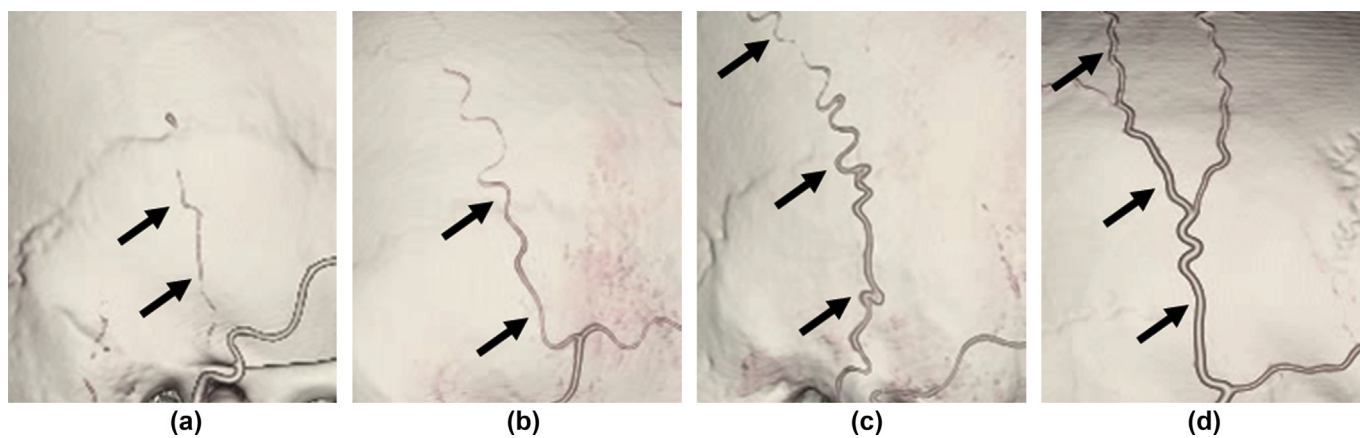
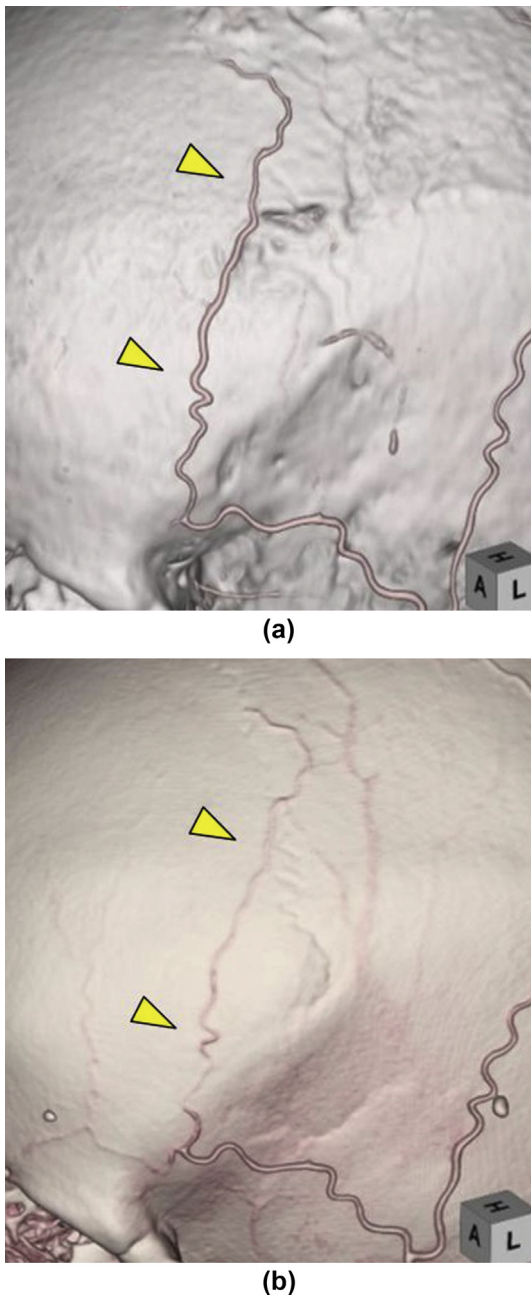


Figure 3 Reference cases of four-grade (0, 1, 2 and 3) system for the evaluation of the parietal branch were presented. (a) Poor depiction (grade 0): almost no depiction of parietal branch (arrow); (b) moderate depiction (grade 1): only the proximal portion was depicted (arrow); (c) good depiction (grade 2): all portions were depicted, but the depiction of the distal portion was observed to be weak (arrow); (d) excellent depiction (grade 3): all parts were well depicted (arrow).



visual assessment. The depiction of STA branches in the CT-based bone–vessel VR images in this study suffered from the beam-hardening effect from the high attenuation value of the skull, resulting in worse image quality. Compared to CTA-based 3D bone–vessel VR imaging, TOF-MRA could achieve a clear depiction of STA branches without beam-hardening artefacts.

A previous report described that the combination of CT as the 3D skull image and TOF-MRA as the 3D angiographic image using the bone–vessel fused image played an important role as a navigation tool for the less invasive surgical procedure of STA-MCA bypass with a minimal incision.¹⁵ Compared to this previous report, the current study achieved 3D bone–vessel VR imaging with superb visibility of STA branches using the non-invasive MRI technique only; this technique will provide sufficient vascular anatomical information as a preoperative assessment for STA-MCA bypass surgery with complete non-invasiveness; however, an extensive manual procedure was part of the reconstruction technique used in the present study in order to obtain black-bone MRI images. This was very time-intensive and must be improved. Notably, bone black signal segmentation may be performed easily by using an automated threshold setting between the black-bone signal and the bright soft-tissue signal around the bone surface. Future work is planned to investigate the improvement in this part of the post-processing technique, which will result in a shortened processing time.

Black-bone MRI acquisition, first described by Eley *et al.*, used the parameter settings of a 3D gradient echo sequence with a proton-density weighted imaging-like contrast.⁶ Their scanning time was described as around 4 minutes. In comparison, the present study used the FIESTA-C sequence of the b-SSFP technique to obtain both high SNR and a shorter scanning time. Recent MRI systems have been developed to allow the parameter settings with much shorter TRs and TEs; such developments could lead to more stable image quality of the b-SSFP sequence. In the current study, acquisition of black-bone MRI was performed successfully with around 3-minute scanning with sufficient VR image visibility. The present FIESTA-C sequence design can be used to achieve almost the same image quality with a short scanning time compared to the previously reported 3D gradient echo sequence technique.^{6–9}

The present study has several limitations. First, it was a retrospective study, and thus there were few patients. Second, the basic sequence of FIESTA-C was used for the acquisition of black-bone MRI to obtain a high SNR image with short scanning time; however, direct comparison to the previously reported method described by Eley *et al.* was not performed. Further analyses to address these limitations will be needed. A third limitation was that source axial images for the evaluation of vessel depiction in both MRI and CT were not used, only 3D reconstructed images were used. A combination of 2D source images and 3D reconstructed fusion images may enable the evaluation of vessel depiction in greater detail. Further analysis will be required to resolve this issue. Fourth, arterial arrival timing of contrast agent in the CTA was determined by focusing on

Figure 4 A case example of marked visualisation difference of STA branches. (a) In the MRI-based bone–vessel fused image, the frontal branch of the STA was well visualised (arrowhead). (b) In contrast, in the CT-based bone–vessel fused image, the same part of the frontal branch was not clearly observed (arrowhead).

Discussion

In the current study, MRI-based 3D skull images could be obtained successfully utilising the signal reverse of 3D FIESTA-C for a 3D VR reconstruction technique. In addition, preoperative bone–vessel VR images for the ICA-ECA bypass were also successfully obtained with the 3D fusion of MRI-based 3D skull images and TOF-MRA. The depiction of STA branches on this MRI-based bone–vessel VR image was deemed superior to that of CT-based images in the

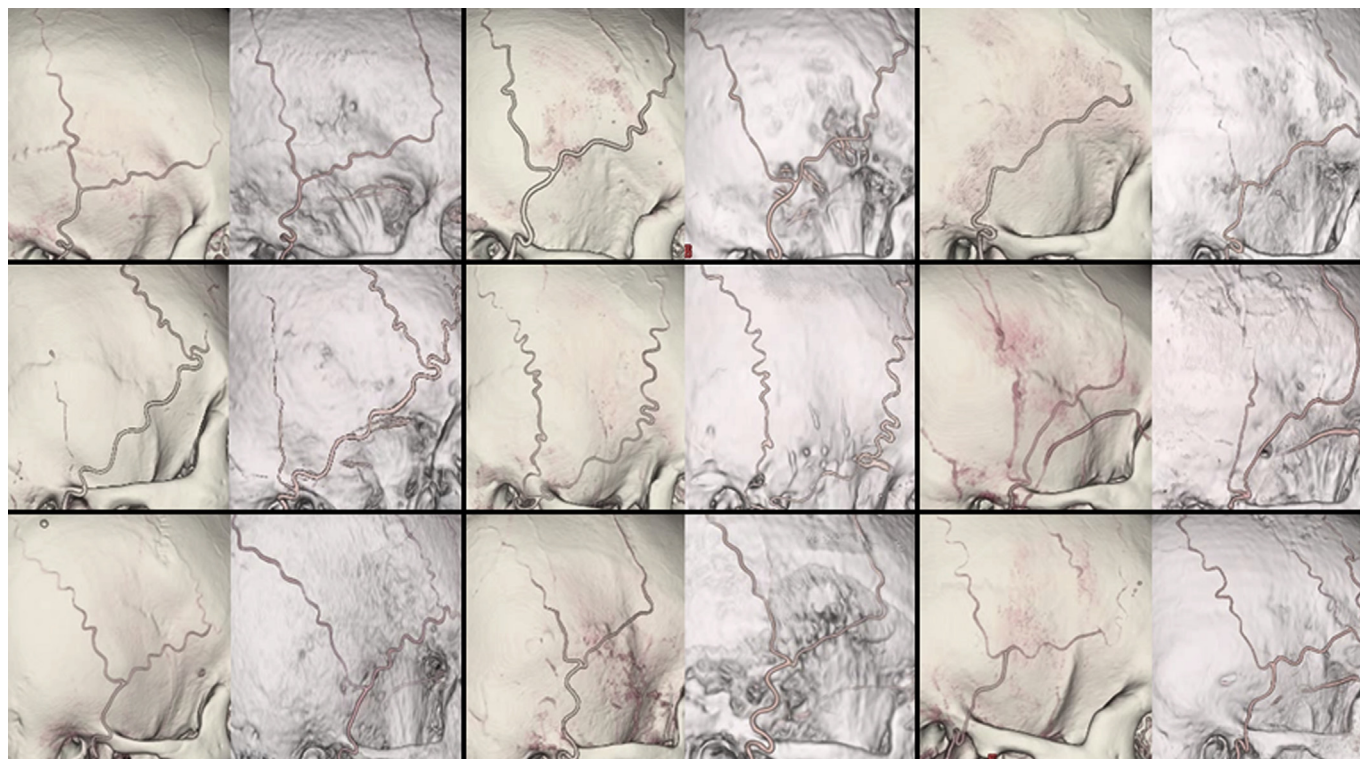


Figure 5 Nine cases of CT-based (left side) and MRI-based (right side) 3D volume-rendering bone-vessel fused images are presented (a–i). Overall, the depiction of the peripheral portion of the STA on MR-based VR images was visually superior to that of CT-based VR.

Table 3

The mean κ values in visual evaluation among raters.

	CT	MR
Frontal branch (right)	0.67	0.60
Parietal branch (right)	0.67	0.76
Frontal branch (left)	0.50	0.65
Parietal branch (left)	0.65	0.60

CT, computed tomography; MRI, magnetic resonance imaging.

the depiction for intracranial arteries. This was slightly different from the best timing for the depiction of branches of the ECA; however, arterial arrival timing between the main trunk of the STA and the peripheral portion of the intracranial arteries was not overly different unless severe stenosis was observed. Additionally, routine head CTA is generally performed to depict the intracranial arteries; depiction of the ECAs is considered optional. CTA acquisition with the best timing of contrast agent arrival to the ECAs is not realistic in daily clinical practice.

In conclusion, MRI bone–vessel fused VR images could be successfully obtained with complete non-invasiveness using FIESTA-C-based black-bone MRI and TOF-MRA. MRI-based bone–vessel VR imaging method was superior for visualising the frontal branches of the STA when compared to the 3D-CTA-based VR imaging method. This technique may be clinically useful for the preoperative evaluation of donor branches for STA-MCA bypass surgery as a non-invasive method.

Conflict of interest

None.

Appendix A. Supplementary data

Supplementary data to this article can be found online at <https://doi.org/10.1016/j.crad.2018.12.019>.

References

1. Batjer H, Mickey B, Samson D. Potential roles for early revascularization in patients with acute cerebral ischemia. *Neurosurgery* 1986;**18**(3):283–91.
2. Onesti ST, Solomon RA, Quest DO. Cerebral revascularization: a review. *Neurosurgery* 1989;**25**(4):618–28. discussion 628–619.
3. Neff KW, Horn P, Dinter D, et al. Extracranial–intracranial arterial bypass surgery improves total brain blood supply in selected symptomatic patients with unilateral internal carotid artery occlusion and insufficient collateralization. *Neuroradiology* 2004;**46**(9):730–7.
4. Nawfel RD, Young GS. Measured head CT/CTA skin dose and intensive care unit patient cumulative exposure. *AJNR Am J Neuroradiol* 2017;**38**(3):455–61.
5. Fushimi Y, Miki Y, Kikuta K, et al. Comparison of 3.0- and 1.5-T three-dimensional time-of-flight MRI angiography in moyamoya disease: preliminary experience. *Radiology* 2006;**239**(1):232–7.
6. Eley KA, McIntyre AG, Watt-Smith SR, et al. "Black bone" MRI: a partial flip angle technique for radiation reduction in craniofacial imaging. *Br J Radiol* 2012;**85**(1011):272–8.
7. Eley KA, Watt-Smith SR, Golding SJ. "Black bone" MRI: a potential alternative to CT when imaging the head and neck: report of eight

- clinical cases and review of the Oxford experience. *Br J Radiol* 2012;**85**(1019):1457–64.
8. Eley KA, Watt-Smith SR, Golding SJ. "Black Bone" MRI: a potential non-ionizing method for three-dimensional cephalometric analysis—a preliminary feasibility study. *Dentomaxillofac Radiol* 2013;**42**(10):20130236.
 9. Eley KA, Watt-Smith SR, Sheerin F, et al. "Black Bone" MRI: a potential alternative to CT with three-dimensional reconstruction of the craniofacial skeleton in the diagnosis of craniosynostosis. *Eur Radiol* 2014;**24**(10):2417–26.
 10. Eley KA, Watt-Smith SR, Golding SJ. Three-dimensional reconstruction of the craniofacial skeleton with gradient echo magnetic resonance imaging ("black bone"): what is currently possible? *J Craniofac Surg* 2017;**28**(2):463–7.
 11. Dremmen MHG, Wagner MW, Bosemani T, et al. Does the addition of a "black bone" sequence to a fast multisequence trauma MRI protocol allow MRI to replace CT after traumatic brain injury in children? *AJNR Am J Neuroradiol* 2017;**38**(11):2187–92.
 12. Scheffler K, Lehnhardt S. Principles and applications of balanced SSFP techniques. *Eur Radiol* 2003;**13**(11):2409–18.
 13. Chavhan GB, Babyn PS, Jankharia BG, et al. Steady-state MRI imaging sequences: physics, classification, and clinical applications. *Radiographics* 2008;**28**(4):1147–60.
 14. Fishman EK, Ney DR. Advanced computer applications in radiology: clinical applications. *Radiographics* 1993;**13**(2):463–75.
 15. Fischer G, Stadie A, Schwandt E, et al. Minimally invasive superficial temporal artery to middle cerebral artery bypass through a mini-craniotomy: benefit of three-dimensional virtual reality planning using magnetic resonance angiography. *Neurosurg Focus* 2009;**26**(5):E20.